Order of the X conduction-band valleys in type-II GaAs/AlAs quantum wells

H. W. van Kesteren and E. C. Cosman
Philips Research Laboratories, P.O. Box 80 000, NL-5600 JA Eindhoven, The Netherlands

P. Dawson, K. J. Moore, and C. T. Foxon
Philips Research Laboratories, Cross Oak Lane, Redhill, Surrey RH1 5HA, England
(Received 6 February 1989)

The optically detected magnetic resonance of electrons and excitons in type-II GaAs/AlAs quantum wells has been studied as a function of the orientation of the quantum well with respect to the direction of the magnetic field. An analysis of the anisotropy reveals that for quantum wells with AlAs layers thinner than ~55 Å the X_z conduction-band valley has the lowest energy while for quantum wells with thicker AlAs layers the X_x and X_y valleys are lowest in energy. This is a consequence of the lattice-mismatch strain splitting of the AlAs X conduction band which dominates the confinement splitting for AlAs layers thicker than ~55 Å.

I. INTRODUCTION

In GaAs/AlAs quantum wells and superlattices both type-I and type-II band alignment can be obtained by an appropriate choice of the layer thicknesses. This is due to the fractional Γ conduction-band offset of ~0.67 and the fact that AlAs is an indirect–band-gap and GaAs a direct–band-gap semiconductor with the lowest conduction band at the X point and Γ point, respectively. When the confinement energy for the electrons in the GaAs layer exceeds the sum of the GaAs-Γ–to–AlAs-X conduction-band offset and the AlAs-X confinement energy, a type-II alignment is obtained with the electrons confined in the AlAs layer and the holes in the GaAs layer (Fig. 1). A crossover occurs for a GaAs thickness of ~35 Å.[1,2] Knowledge of the band structure of type-II GaAs/AlAs structures that are indirect in position as well as in momentum space is of interest because the direct–band-gap type-I to indirect–band-gap type-II crossover might be useful in electro-optic devices[3] and because of similarities to the $GaAs_{1-x}P_x$/GaP and $Si_{1-x}Ge_x$/Si systems.

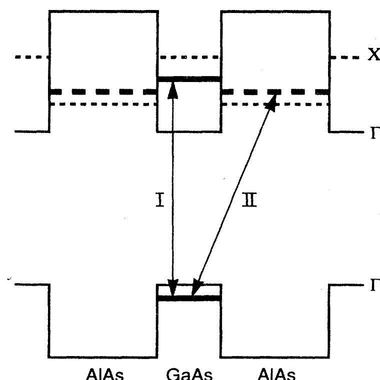

FIG. 1. Band structure for GaAs/AlAs quantum wells showing the type-I and -II transitions. The subbands are indicated by the thick lines.

In bulk AlAs the lowest X conduction band is threefold degenerate at the band edge, corresponding to the symmetry-equivalent $(2\pi/a)$ (1,0,0) points in the Brillouin zone. However, in quantum wells and superlattices this degeneracy is lifted due to confinement and strain. Confinement splits the X valley with momentum vector **k** parallel to the growth direction (labeled X_z) apart from the X valley with **k** vector in the quantum-well plane (X_x and X_y). In the literature, considerable controversy exists as to whether the X_z or the X_x and X_y valley are lowest in energy.[4–14] The confinement energy for the electrons in the X_z valley, which have a component of momentum along the growth direction, is determined by the longitudinal effective mass while the confinement for the X_x and X_y valleys is determined by their transverse effective mass which is about six times smaller. We therefore anticipate that due to confinement the X_z valley would have the lowest energy. This is in agreement with envelope-function calculations[4,5] and the one-band Wannier orbital calculation of Ting and Chang.[6] However, the tight-binding calculations by Ihm[7] predict that the order is reversed for AlAs layers thinner than ~20 Å. All these calculations neglected the effect of strain on the conduction-band structure. Because the lattice constant of AlAs is larger than that of the GaAs substrate, the AlAs layers are under biaxial compression. The lattice mismatch strain results in a lowering of the X_x and X_y valleys with respect to the X_z valley.[15] Recently, Drummond *et al.*[15] pointed out that the confinement and strain splittings are of comparable magnitude.

Photoluminescence (PL) and decay characteristics also provide conflicting results. The PL lines observed by Moore *et al.*[8,9] were attributed to exciton recombination involving X_z electrons, while similar spectra of Finkman *et al.*[10,11] were interpreted as due to the recombination of excitons involving X_x and/or X_y electrons. The nonexponential decay of the type-II luminescence as observed

 ©1989 The American Physical Society

by Finkman and co-workers was used to support their idea of X_x and/or X_y excitons. Later, Minami *et al.*[12] questioned their analysis and concluded that the nonexponential character could be explained by the recombination of excitons involving X_z electrons. Recently, Dawson and co-workers[13] studied the decay rates as a function of the AlAs thickness. The variation of the decay rates could be explained by a change in the mixing between the AlAs-X_z and GaAs-Γ electron states caused by the discontinuity at the heterointerface. Uniaxial stress measurements by Gil *et al.*[14] also supported the idea that in thin GaAs/AlAs quantum wells the X_z valley has the lowest energy.

In a previous paper[16] we reported that the type-II GaAs/AlAs quantum wells can be studied by use of the optically detected magnetic resonance (ODMR) technique and interpreted the various resonance lines. In this paper we will analyze the anisotropy of the ODMR spectra as a function of the orientation of the magnetic field with respect to the quantum-well axes. It will be shown that the ordering of the X_x and/or X_y and X_z valleys can be obtained from the anisotropy and that their respective energies cross for an AlAs layer thickness of ~ 55 Å. A preliminary analysis of a part of the anisotropy data has been given in Ref. 17.

II. RESULTS AND ANALYSIS

The samples used in this study were grown by molecular-beam epitaxy (MBE). The layers were deposited on (001)-oriented GaAs substrates at a temperature of 630–650 °C and consisted of 1.0 μm of GaAs buffer material, 60–1740 periods of GaAs/AlAs, where the number depends on the thickness of the layers and finally a capping layer of 0.1 μm of GaAs. The GaAs and AlAs thicknesses for the various samples are given in Table I. For one series of samples investigated, the GaAs thickness was fixed at nominally 25 Å and the AlAs thickness varied between 17 and 200 Å. For the other series, the GaAs and AlAs thicknesses were equal and varied between 3 and 6 monolayers (8 and 17 Å) for the various samples. The ODMR experiments were carried out at 9.68 GHz with the sample at a temperature of 1.6 K. For excitation, the 514-nm line from an argon-ion laser was used. The luminescence was detected in a direction parallel to the magnetic field while the sample could be rotated around an axis perpendicular to the field. The ODMR spectra were recorded with phase-sensitive detection of the difference between the two circularly polarized components of the luminescence using a photoelastic modulator operating at 50 kHz.

The type-II PL features for two samples consisting of (25 Å GaAs)/(25 Å AlAs) and (25 Å GaAs)/(76 Å AlAs), respectively, are shown in Fig. 2. The PL spectra for the samples with AlAs thicknesses from 17 up to 42 Å have similar shapes, showing one intense line with two weaker lines at lower energy. For the 8, 11, and 14 Å $(GaAs)_n/(AlAs)_n$ samples the PL spectra look quite different, showing three distinct lines with comparable intensity. The PL spectra of the samples with AlAs thicknesses up to 42 Å are discussed in the papers by Moore *et al.*[8,9] The samples with AlAs layers thicker than 42 Å generally show three intense lines and several weaker lines. All these lines become broader and start to overlap for the thickest AlAs layer samples. To obtain more information on the origin of the PL lines, the ODMR spectra and their dependence on the orientation of the quantum-well axes with respect to the magnetic field direction have been studied. Two representative ODMR spectra for the magnetic field parallel to the [001] axis are shown in Fig. 3. These spectra were obtained by monitoring all the type-II luminescence. The angular

TABLE I. Sample identifier, nominal GaAs and AlAs thickness (the number in parentheses is the thickness as obtained from x-ray diffraction combined with photoluminescence excitation spectroscopy), g values, and lowest X valley(s). The error in the g values is ± 0.01.

Sample	GaAs (Å)	AlAs (Å)	g_{xx}^{II}	g_{yy}^{II}	g_{zz}^{II}	X_x, X_y, X_z
No. 1 (G344)	8	8	$>g_{zz}$	$>g_{zz}$	1.92	X_z
No. 2 (G343)	11	11	$>g_{zz}$	$>g_{zz}$	1.91	X_z
No. 3 (G345)	14	14	$>g_{zz}$	$>g_{zz}$	1.91	X_z
No. 4 (G340)	17	17	$>g_{zz}$	$>g_{zz}$	1.90	X_z
No. 5 (G264)	25(22)	17(19)	1.99	1.99	1.89	X_z
No. 6 (G261)	25(23)	25(28)	1.99	1.99	1.89	X_z
No. 7 (G262)	25(23)	42(41)	1.99	1.99	1.88	X_z
No. 8 (G170)	25	68			1.99	X_x, X_y
No. 9 (G510)	25	76	1.94	1.94	1.99	X_x, X_y
No. 10 (512)	25	100	1.89	1.99	1.99	X_x, X_y
			1.99	1.89	1.99	
No. 11 (G515)	25	120	1.89	1.99	1.99	X_x, X_y
			1.99	1.89	1.99	
No. 12 (G517)	25	150	1.89	1.99	1.99	X_x, X_y
			1.99	1.89	1.99	
No. 13 (G519)	25	200	1.89	1.99	1.99	X_x, X_y
			1.99	1.89	1.99	

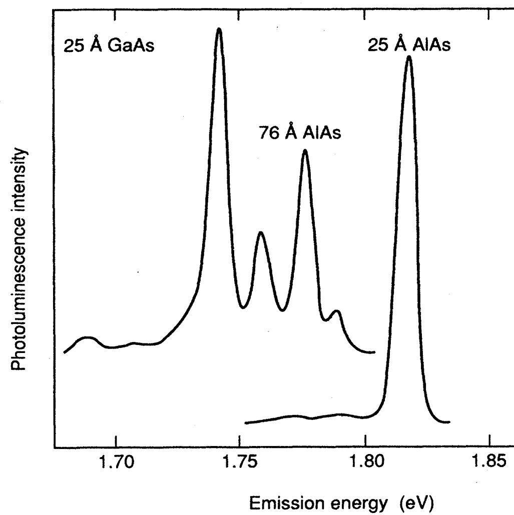

FIG. 2. Low-temperature (1.6 K) photoluminescence spectra of the (25 Å GaAs)/(25 Å AlAs) and (25 Å GaAs)/(76 Å AlAs) samples.

dependence of the resonance fields for several samples are shown in Figs. 4(a)–4(c).

In Ref. 16 it was shown that the outer two ODMR lines for the (25 Å GaAs)/(25 Å AlAs) sample correspond to electron-spin transitions in the heavy-hole exciton and that they are split apart by the exchange interaction of the electron and the hole. The resonance line in between was ascribed to the unbound electrons in the AlAs layer. The exchange spitting obtained from the ODMR experiments for samples with various GaAs and AlAs thicknesses has been discussed by Rejaei Salmassi and Bauer.[18] For the samples with 25 Å GaAs and AlAs lay-

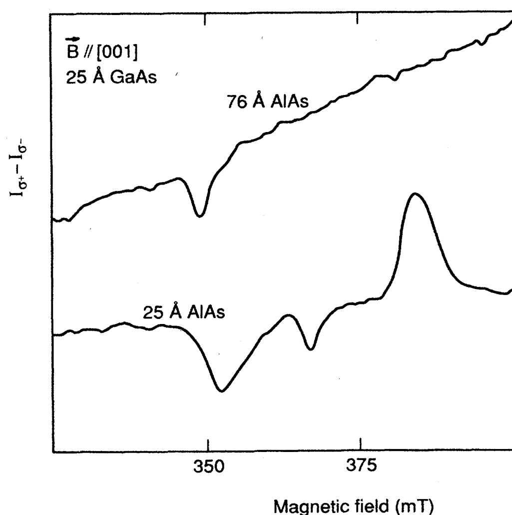

FIG. 3. ODMR spectra of the (25 Å GaAs)/(25 Å AlAs) and (25 Å GaAs)/(76 Å AlAs) samples. The spectra have been recorded by detecting the difference of the two circularly polarized components σ^+ and σ^- of all the type-II luminescence.

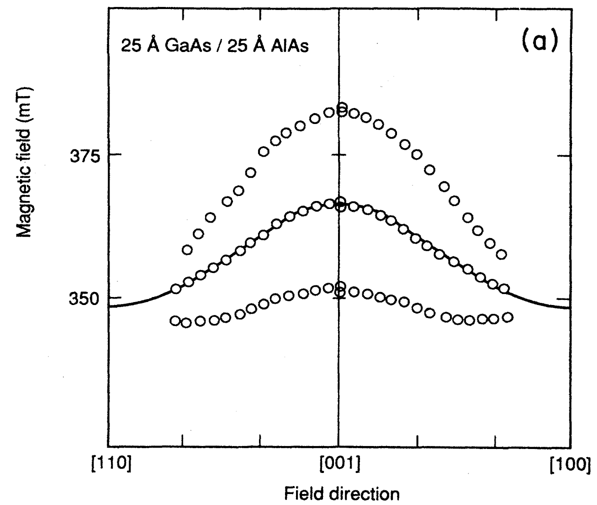

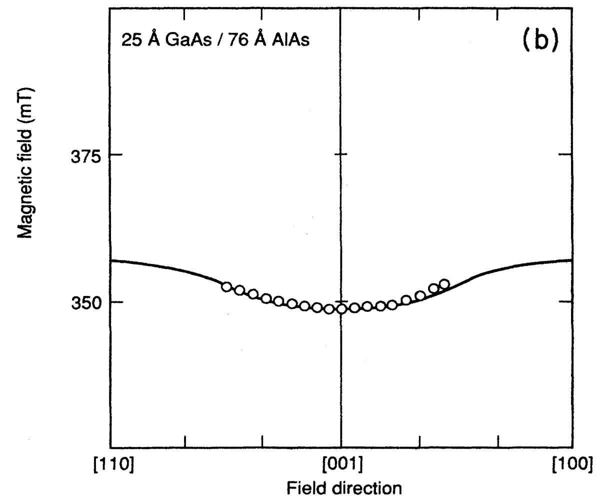

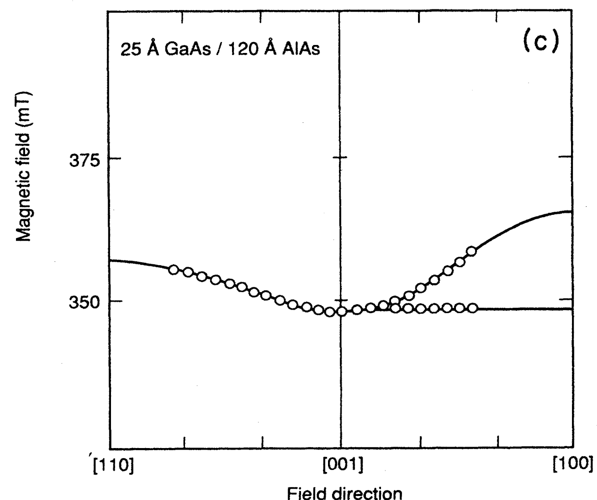

FIG. 4. Angular dependence of the ODMR spectra for (a) the (25 Å GaAs)/(25 Å AlAs), (b) the (25 Å GaAs)/ (76 Å AlAs), and (c) the (25 Å GaAs)/(120 Å AlAs) sample.

ers thicker than ~50 Å the exchange splitting is no longer resolved. The ODMR spectra, apart from the exchange splitting which is not relevant for the present analysis, can be described by the spin Hamiltonian for electrons with spin $S=\frac{1}{2}$, given by

$$H_e=\mu_B(g_{xx}B_xS_x+g_{yy}B_yS_y+g_{zz}B_zS_z) , \quad (1)$$

where the g value is written as a tensor having only diagonal elements g_{xx}, g_{yy}, and g_{zz} with x,y,z corresponding, respectively, to the [100], [010], and [001] crystal axes, μ_B is the Bohr magneton, and **B** the magnetic field. The g values, obtained for the various samples by fitting the eigenvalues of the spin Hamiltonian matrix to the angular dependence of the resonance fields, are shown in Table I. For the samples that show both an electron-spin resonance and exchange-split exciton resonances, the g values have been obtained from the angular dependence of the electron-spin resonance field only. When the exchange interaction matrix is included, however, the angular dependence of the exciton resonance fields in these samples can be fitted using the same electron-spin g values.[17,19] For the samples with AlAs layers thicker than or equal to 100 Å, the spectra have to be described by two **g** tensors.

To relate these g values to the band structure we have to consider the electron and exciton wave functions. For bulk AlAs the proper X valley electron states are the even (symmetry X_1) and odd (symmetry X_3) combinations of the minima on the same axis. The origin is thereby taken to be at an As site.[20] The X_1-X_3 splitting amounts to ~0.5 eV with X_1 the lowest band.[20,21] Due to confinement and strain the threefold degeneracy of the X_1 and X_3 bands is partially lifted in quantum wells. These splittings however, are small compared to the bulk X_1-X_3 splitting. In the effective-mass approximation the X electron and type-II exciton wave functions can be written as a linear combination of degenerate wave functions corresponding to the equivalent X minima

$$\Psi^j_{\rm el}(\mathbf{r}_e)=\sum_i \alpha^j_i\psi^c_i(\mathbf{r}_e) , \quad (2)$$

$$\Psi^j_{\rm exc}(\mathbf{r}_e,\mathbf{r}_h)=\Omega^{2/3}\sum_i \alpha^j_iF_i(\rho,z_e,z_h)\psi^c_i(\mathbf{r}_e)\psi^v(\mathbf{r}_h) . \quad (3)$$

The arguments $\mathbf{r}_e$ and $\mathbf{r}_h$ are the coordinates of the electron and hole and $\rho=(x_e,y_e)-(x_h,y_h)$ denotes the difference coordinates in the plane. ψ^v and ψ^c_i denote the Bloch functions of the Γ valence-band holes and the X conduction-band electrons, where i is taken to correspond to the six minima located at $(k_X,0,0)$, $(-k_X,0,0),\ldots,(0,0,-k_X)$. F_i is the ground-state exciton envelope function for the uncoupled valleys, j indexes the different linear combinations, and Ω is the total volume of the system. The coefficients α^j_i and the degeneracy which remains can be ascertained from symmetry without detailed knowledge of the nature of the perturbations.[22] For the analysis of the ODMR experiments only the lowest energy states which are derived from the bulk X_1 band have to be considered. For the D_{2d} symmetry of the quantum well we obtain, for these X_1-derived states,

$$X_{xy}(A_1):\ \alpha=\tfrac{1}{2}(1,1,1,1,0,0) , \quad (4a)$$

$$X_{xy}(B_1):\ \alpha=\tfrac{1}{2}(1,1,-1,-1,0,0) , \quad (4b)$$

$$X_z(A_1):\ \alpha=\tfrac{1}{2}\sqrt{2}(0,0,0,0,1,1) . \quad (4c)$$

The various states are labeled according to the X minima involved and their transformation properties are indicated in the parentheses. Anticipating the discussion of the experimental results we also consider the electron and exciton states in the lower D_2 symmetry which are given by

$$X_x(A_1):\ \alpha=\tfrac{1}{2}\sqrt{2}(1,1,0,0,0,0) , \quad (5a)$$

$$X_y(A_1):\ \alpha=\tfrac{1}{2}\sqrt{2}(0,0,1,1,0,0) , \quad (5b)$$

$$X_z(A_1):\ \alpha=\tfrac{1}{2}\sqrt{2}(0,0,0,0,1,1) . \quad (5c)$$

The g value for the electrons on a single ellipsoidal energy surface is anisotropic and differs from the free electron g value as a result of spin-orbit interaction. From symmetry the **g** tensor, e.g., for the $(0,0,k_X)$ minimum, has only the components $g_{xx}=g_{yy}=g_t$ and $g_{zz}=g_l$, where the z axis is the principal axis of the ellipsoid. The **g** tensors for the X electrons and type-II excitons are now obtained by summing up the contributions from the different minima:

$$\mathbf{g}^j=\sum_i(\alpha^j_i)^2\mathbf{g}_i , \quad (6)$$

where $\mathbf{g}_i$ is the **g** tensor for the ith minimum. Assuming that the magnitude of g_t and g_l does not differ for the various minima, the **g** tensors for the states given in Eqs. (4) and (5) can be compared. For the D_{2d}, $X_{xy}(A_1)$, and $X_{xy}(B_1)$ states we obtain $g_{xx}=g_{yy}=\frac{1}{2}(g_l+g_t)$, $g_{zz}=g_t$, while for the $X_z(A_1)$ state we find $g_{xx}=g_{yy}=g_t$, $g_{zz}=g_l$. So both X_{xy} and X_z states show a uniaxial symmetry along the [001] axis. The total anisotropy is given by $\Delta g=g_{zz}-g_{xx}=-\frac{1}{2}(g_l-g_t)$ for the X_{xy} states and $\Delta g=g_{zz}-g_{xx}=g_l-g_t$ for the X_z state. For the D_2-symmetry X_x,X_y,X_z states the Zeeman splitting shows a uniaxial symmetry along an axis which corresponds to the principal axis of the valley involved while the anisotropy equals $\Delta g=g_l-g_t$ for all three states.

From the symmetry axis, the number of spin resonances observed, and the difference in magnitude of the anisotropy for the X_{xy} and X_z states, the ordering of the X valleys in the various samples can be determined without knowledge of the exact value of g_l and g_t. For instance, when we compare the angular dependence of the ODMR signals of the (25 Å GaAs)/(25 Å AlAs) with the (25 Å GaAs)/(120 Å AlAs) sample [Figs. 4(a) and 4(c)], it is clear that the anisotropy for the first sample has a [001] uniaxial symmetry and can be described by one **g** tensor while the anisotropy for the second sample has to be described by two **g** tensors with uniaxial symmetry axes [100] and [010], respectively. Therefore, the X_z valley is lowest in energy in the 25-Å AlAs sample and the X_x and X_y valleys in the 120-Å AlAs sample. Considering Eqs. (4) and (5), the symmetry for the electron exciton states in the 25-Å AlAs sample can both be D_{2d} or D_2; however, the observation of both X_x and X_y states in

the 120-Å sample is only compatible with a D_2 symmetry. For the (25 Å GaAs)/(76 Å AlAs) sample the magnitude and the sign of the anisotropy indicate that in this sample a D_{2d}-symmetry–mixed X_{xy} state is observed.

In Table I the g values and the results with respect to the ordering of the valleys are given for all the samples studied. Considering the g values, it is clear that within the experimental accuracy the magnitude of g_l and g_t is independent of the valley and thickness of the layers for nearly all samples. Only for the thinnest quantum-well samples is a slight increase found of $g_{zz}=g_l$. This makes it possible to determine the ordering of the X valleys in all the samples. For the samples with AlAs layer thicknesses ≤ 42 Å the X_z valley has the lowest energy while for the samples with AlAs thicknesses ≥ 68 Å the X_x and/or X_y valleys are lowest.

III. DISCUSSION

To determine whether this crossover of the X_z and X_x and/or X_y valleys is due to misfit strain, the effect of and the strain on the X conduction band has to be considered.[15] The multiple-quantum-well structures studied have been grown on GaAs substrates. Therefore, the GaAs layers are presumably unstrained and all the strain is found in the AlAs layers. The in-plane strain is determined by the low-temperature lattice constants of GaAs and AlAs (Refs. 21 and 23):

$$e_{\parallel}=e_{xx}=e_{yy}=\frac{a_{\mathrm{GaAs}}-a_{\mathrm{AlAs}}}{a_{\mathrm{AlAs}}}=-1.8\times10^{-3}, \quad (7)$$

while the perpendicular expansion is given by

$$e_{\perp}=e_{zz}=-2\frac{C_{12}}{C_{11}}e_{\parallel}=1.7\times10^{-3}, \quad (8)$$

where the C_{ij} are the AlAs elastic stiffness constants.[24] The low-temperature lattice constant of AlAs is not known and has therefore been calculated from the temperature dependence of the coefficient of linear expansion.[23] The low-temperature strains given in Eqs. (7) and (8) are about 5% larger than the ones calculated for room temperature and about 15% larger than those obtained from x-ray diffraction by Kamigaki *et al.*[25] The change in the volume of the unit cell results in a shift of all the X valleys of a few meV while the Ξ_u component of the deformation potential gives rise to a splitting of the X_x and/or X_y and X_z valleys by

$$\Delta X=\Xi_u(e_{\perp}-e_{\parallel}). \quad (9)$$

The AlAs deformation potential is also not known; however, the deformation potentials for GaP and GaAs are the same,[21,26] indicating that they do not differ much for the various III-V compound semiconductors. Using the GaP/GaAs deformation potential $\Xi_u=6.5$ eV, we obtain as an estimate for the valley splitting $\Delta X=23$ meV.

This value should be compared with the energy difference of the X_x and/or X_y and X_z subbands. The subband energies have been calculated within the envelope function approximation. The calculations were made using longitudinal and transverse X point masses of $1.3m_0$ and $0.19m_0$, respectively. The results are shown in Fig. 5. When we compare the confinement and strain effects the difference in the X_z and X_x and/or X_y exciton binding and localization energies should also be taken into account. For the X_z excitons the binding energy has recently been calculated by Rajaei Salmassi and Bauer.[18] Similar calculations for the X_x and/or X_y excitons show that their binding energy is ~ 1 meV larger. This number depends slightly on the layer thicknesses and the choice of the in-plane mass which is built up of both longitudinal and transverse masses. The number given has been calculated for a (25 Å GaAs)/(50 Å AlAs) sample and an average in-plane mass of $2(1/m_t+1/m_l)^{-1}=0.3m_0$. The localization energy for both the X_x and/or X_y and X_z excitons is mainly determined by the hole localization energy due to the larger slope of the confinement energy versus well thickness for the holes compared to the electrons in the samples studied. So, the X_x and/or X_y and X_z exciton localization energies are expected to be similar. The correction for the binding as well as for the localization energy is therefore small compared to the 23-meV strain splitting and not relevant for the present analysis. From the calculated strain splitting and subband energies we expect a crossing at about 60 Å, which is in good agreement with the ODMR result.

Our experimental evidence that the X_z valley has the lowest energy in thin type-II GaAs/AlAs structures with layers as thin as 8 Å contradicts the result from the tight-binding calculations of Ihm.[7] It should be noted that band mixing effects and, e.g., the Bloch components of the X conduction band are ignored in the envelope function approach. One way to overcome this problem is to use a microscopic technique such as the tight-binding formalism. However, a difficulty in these tight-binding calculations is that only nearest-neighbor parameters are

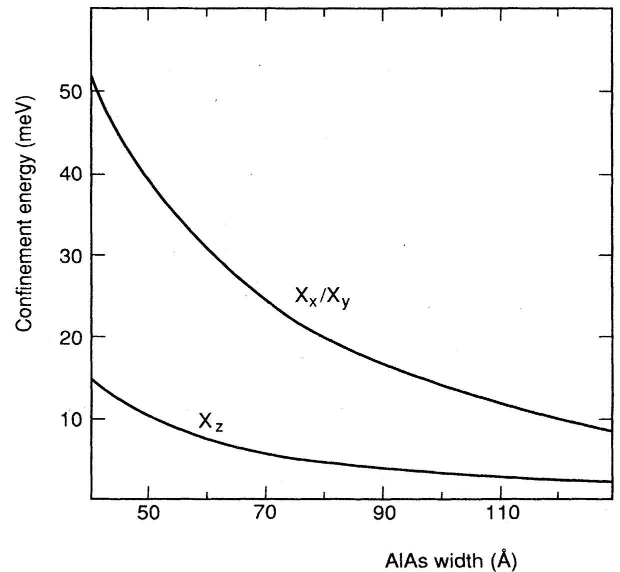

FIG. 5. Subband energy for the X_x and/or X_y and the X_z valleys as obtained from an envelope function calculation.

included. As noted by Ting and Chang,[6] these calculations consequently suffer from having an infinite transverse X-valley mass, giving inevitably the X_x and X_y valleys the lowest subband energy. This is most likely the origin of the discrepancy between our results and the tight-binding result.

Other microscopic methods applied to thin GaAs/AlAs structures are, e.g., the one-band Wannier orbital model as used by Ting and Chang[6] and the linearized augmented plane wave method used by Wei and Zunger.[27] Although the envelope function results for the ordering of the X_x and/or X_y and X_z valleys agree with the ODMR results for samples with GaAs and AlAs layers as thin as 8 Å, we will take a closer look at these microscopic models because they can provide more information on, e.g., the mixing and splitting of the various conduction-band states.

For a (001) GaAs/AlAs superlattice the bulk Γ, X_x and X_y states correspond to the superlattice $\Gamma(000)$, $M_x(100)$, and $M_y(010)$ states while the X_z state is folded into the superlattice Γ state and the X_x and X_y states into the M_y and M_x states, respectively. The folding of, e.g., the X_x state into the M_y state is due to the fact that the $X_x(100)$ point is equivalent to the (011) point in k space because they differ by the reciprocal lattice vector $(\bar{1}11)$. This means that both the GaAs-Γ and AlAs-X_z states as well as the AlAs-X_x and -X_y states can be mixed. According to Ting and Chang[6] and Wei and Zunger[27] the magnitude of this mixing depends on the parity of the states. For instance, the X_z state can be written as an envelope function which is symmetric with respect to the well center modulated by a phase factor $\cos(k_X z)$ with the origin at an As site. If the AlAs slab consists of an odd number of monolayers the parity of the Bloch functions with respect to the well center and the subband envelope function parity are both even, which makes mixing with even the lowest Γ subband allowed. However, for an even number of AlAs layers the overall parity of the X_z and Γ states is different and mixing is not allowed. Therefore Γ-X_z and similarly X_x-X_y mixing by the superlattice potential only occurs for AlAs slabs with an odd number of monolayers.

The X_x-X_y mixing by the superlattice potential gives rise to a splitting of the $X_{xy}(A_1)$ and $X_{xy}(B_1)$ states. For these D_{2d} symmetry states, the magnitude of the X_x-X_y mixing cannot be obtained from the ODMR experiment because the spectra are always described by the same **g** tensor. However, from Table I it is clear that in all the samples where the X_x and X_y valleys have the lowest energy, the relevant symmetry is not D_{2d} but D_2, with exception of the (25 Å GaAs)/(76 Å AlAs) sample where the symmetry is D_{2d}. This means that in all the samples with AlAs thicknesses ≥ 100 Å a perturbation exists which splits the X_x and X_y states apart and which is larger than the X_x-X_y mixing potential. An upper limit for the X_x-X_y mixing potential can be obtained from the intensity ratio of the X_x and X_y ODMR signals assuming that the populations of these two states are in thermal equilibrium. The largest ratio observed in the samples with AlAs layers ≥ 100 Å was about 0.3. Furthermore, we noticed that the intensity ratio varies slightly when scanning the laser beam over the sample. This variation is compatible with a Boltzmann population distribution and a slightly varying splitting of the X_x and X_y states over the sample. The observation that the X_x and X_y signals have at least an intensity ratio of ~ 0.3 thus shows that the X_x-X_y mixing potential is smaller than ~ 0.2 meV. It is unlikely that all the samples with AlAs layer thicknesses ≥ 100 Å have only AlAs layers consisting of an even number of monolayers where no mixing by the superlattice potential occurs. Therefore the 0.2 meV is also an upper limit for the superlattice potential mixing in these quantum wells. For the (25 Å GaAs)/(76 Å AlAs) sample a D_{2d} symmetry is observed in the ODMR experiments. So the mixing potential in this sample is larger or comparable to the X_x-X_y splitting. Indeed, if the X_x-X_y mixing is due to the superlattice potential, it should increase for decreasing layer thicknesses of the quantum well giving mixed X_{xy} states for the thinner type-II quantum wells. For the quantum wells with AlAs thicknesses smaller than ~ 55 Å the X_z valley becomes lowest in energy and the X_x-X_y mixing is no longer relevant.

For the samples where the X_z state is lowest the anisotropy of the ODMR signals does not provide enough information to reveal whether the symmetry is D_{2d} or lower. However, recent quantum beat experiments by van der Poel *et al.*[28] and zero-field ODMR experiments[19] showed that the axial symmetry in these quantum wells is also lifted. The origin of the lowering of the D_{2d} symmetry is not quite clear at the moment. An in-plane strain can split the X_x and X_y states; however, the lowering of the symmetry can also be due to the fact that the GaAs/AlAs interface plays and important role in the microscopic structure of the type-II excitons.

We now turn to the PL spectra shown in Fig. 2. For the samples with AlAs layers thinner than ~ 55 Å the X_z state has the lowest energy. Due to the mixing of the X_z state with the Γ state the k conservation rule is broken. This gives rise to an intense zero-phonon line and weaker phonon lines at lower energy. According to the energy spacings of 30 and 50 meV, the phonons involved are identified as LA and LO AlAs phonons.[9] For the samples with the thicker AlAs layers where the X_x and/or X_y states are lowest there is no mixing with the Γ states, and in principle only phonon-assisted decay is allowed. We therefore expect several intense phonon lines in the spectrum. To reveal whether the three main lines in the PL spectra have a common origin, the ODMR spectrum for the (25 Å AlAs)/(76 Å GaAs) has been recorded with wavelength-selective detection. This experiment showed that the three main lines in the spectrum give the same ODMR spectrum and therefore have the same origin. The other lines in the spectra were too weak for this experiment to be performed. The energy spacing of these lines with respect to the weaker higher-energy line is constant for the samples with different AlAs thicknesses and amounts to 14, 32, and 50 meV. We therefore interpret the weak highest-energy line as the zero-phonon line and the other lines as the TA-, LA-, and LO-phonon recom-

bination lines of X_x and/or X_y states. This interpretation is in accordance with a much stronger temperature dependence in the 2–10-K range for the intensity of the zero-phonon line with respect to the phonon lines. This strong temperature dependence indicates a breaking of the k selection rule by interface scattering, which becomes important when the excitons that are localized at low temperature at the interface fluctuations become mobile at higher temperatures. The small lines at lower energy correspond to 2–LO- and (LO+TA)-phonon lines.

In the PL spectra of the 100 and 120 Å AlAs samples another weak line is observed at an energy, 9 and 14 meV respectively, above the zero-phonon X_x and/or X_y recombination line. The energy difference of this line with respect to the X_x and/or X_y line corresponds fairly well to the value obtained for an X_z line from the combined effect of confinement and strain as calculated above. The observation of this PL line thus lends extra support to the analysis given. A detailed PL and PL excitation study of the thick ALAs layer samples will be the subject of a forthcoming publication.[29]

IV. CONCLUSIONS

It has been shown that both confinement and strain should be considered to describe the conduction-band structure of type-II GaAs/AlAs quantum wells. For samples with AlAs layers thinner than ~55 Å the confinement effect dominates, giving the X_z valley the lowest energy, whereas for samples with AlAs layers thicker than ~55 Å the strain effect dominates, giving the X_x and X_y valleys the lowest energy. In the samples with AlAs layer thicknesses ≥100 Å the X_x and X_y valleys are also split apart. This splitting is, however, much smaller than the X_x and/or X_y to X_z splitting. The splitting of the X_x and X_y states shows that the actual symmetry is lower than the anticipated D_{2d} symmetry for quantum wells. The ODMR technique is a powerful technique to reveal this and to facilitate the interpretation of the various luminescence lines in the type-II PL spectra.

ACKNOWLEDGMENTS

We are indebted to G.E.W. Bauer for calculating the difference of the X_z and X_x and/or X_y exciton binding energy and to D. J. Hilton for assistance with the MBE growth.

[1]G. Danan, B. Etienne, F. Mollot, R. Planel, A. M. Jean-Louis, F. Alexandre, B. Jusserand, G. Le Roux, J. Y. Marzin, H. Savary, and B. Sermage, Phys. Rev. B **35**, 6207 (1987).

[2]P. Dawson, K. J. Moore, and C. T. Foxon, in *Proceedings of the Conference on Quantum Wells and Superlattice Physics*, Vol. 792 of *SPIE Proceedings* (International Society of Photo-Optical Instrumentation Engineers, Bellingham, WA, 1987), p. 208.

[3]M. H. Meynadier, R. E. Nahory, J. M. Worlock, M. C. Tamargo, J. L. de Miguel, and M. D. Sturge, Phys. Rev. Lett. **60**, 1338 (1988).

[4]P. P. Ruden, D. C. Engelhardt, and J. K. Abrokwah, J. Appl. Phys. **61**, 294 (1987).

[5]G. Duggan, and H. I. Ralph, in Ref. 2, p. 147.

[6]D. Z.-Y. Ting and Yia-Chung Chang, Phys. Rev. B **36**, 4359 (1987).

[7]J. Ihm, Appl. Phys. Lett. **50**, 1068 (1987).

[8]K. J. Moore, G. Duggan, P. Dawson, and C. T. Foxon, Phys. Rev. B **38**, 5535 (1988).

[9]K. J. Moore, P. Dawson, and C. T. Foxon, Phys. Rev. B **38**, 3368 (1988).

[10]E. Finkman, M. D. Sturge, and M. C. Tamargo, Appl. Phys. Lett. **49**, 1299 (1986).

[11]E. Finkman, M. D. Sturge, M. H. Meynadier, R. E. Nahory, M. C. Tamargo, D. M. Hwang, and C. C. Chang, J. Lumin. **39**, 57 (1987).

[12]F. Minami, K. Hirata, and K. Era, Phys. Rev. B **36**, 2875 (1987).

[13]P. Dawson, K. J. Moore, C. T. Foxon, and G. W. 't Hooft, J. Appl. Phys. (to be published).

[14]B. Gil, P. Lefebvre, H. Mathieu, F. Mollot, and R. Planel, in *Proceedings of the 19th International Conference on the Physics of Semiconductors*, edited by W. Zawadzki and J. M. Langer (Institute of Physics, Polish Academy of Sciences, Warsaw, 1988), p. 365.

[15]T. J. Drummond, E. D. Jones, H. P. Hjalmarson, and B. L. Doyle, in *Proceedings of the Conference on the Growth of Compound Semiconductors*, Vol. 796 of *SPIE Proceedings* (International Society of Photo-Optical Instrumentation Engineers, Bellingham, WA, 1987), p. 2.

[16]H. W. van Kesteren, E. C. Cosman, F. J. A. M. Greidanus, P. Dawson, K. J. Moore, and C. T. Foxon, Phys. Rev. Lett. **61**, 129 (1988).

[17]H. W. van Kesteren, E. C. Cosman, P. Dawson, K. J. Moore, and C. T. Foxon, Ref. 14, p. 239.

[18]B. Rejaei Salmassi and G. E. W. Bauer, Phys. Rev. B **39**, 1970 (1989).

[19]H. W. van Kesteren, W. A. J. A. van der Poel, E. C. Cosman, and C. T. Foxon (unpublished).

[20]R. M. Wentzcovitch, M. Cardona, M. L. Cohen, and N. E. Christensen, Solid State Commun. **67**, 927 (1988).

[21]*Landolt-Börnstein, Numerical Data and Functional Relationships in Science and Technology, New Series III/17a*, edited by O. Madelung, M. Schultz, and H. Weiss (Springer-Verlag, Berlin, 1982).

[22]F. Bassani, G. Iadonisi, and B. Preziosi, Rep. Prog. Phys. **37**, 1099 (1974).

[23]N. N. Sirota, A. M. Antuyukhov, and A. A. Sidorov, Dokl. Akad. Nauk SSSR **277**, 1397 (1984) [Sov. Phys.—Dokl. **29**, 662 (1984)].

[24]S. Adachi, J. Appl. Phys. **58**, R1 (1985).

[25]K. Kamigaki, H. Sakashita, H. Kato, M. Nakayama, N. Sano,

and H. Terauchi, Appl. Phys. Lett. **49**, 1071 (1986).
[26]D. N. Mirlin, V. F. Sapega, I. Ya. Karlik, and R. Katilius, Solid State Commun. **61**, 799 (1987).
[27]S. H. Wei and A. Zunger, J. Appl. Phys. **63**, 5794 (1988).
[28]W. A. J. A. van der Poel, A. L. G. J. Severens, and C. T. Foxon (unpublished).
[29]P. Dawson, K. J. Moore, C. T. Foxon, and H. W. van Kesteren (unpublished).